CrossMark

ORIGINAL ARTICLE

Green and Selective Fluorescent Sensor for Detection of Sn (IV) and Mo (VI) Based on Boron and Nitrogen-Co-Doped Carbon Dots

Reza Tabaraki[1] · Omran Abdi[1] · Sedigheh Yousefipour[1]

Abstract A green and simple microwave-assisted method was used to synthesis water-soluble boron and nitrogen-co-doped carbon dots (B-N-CDs). These B-N-CDs were successfully used for the fluorescent determination of Sn^{4+} and Mo^{6+} ions. This probe had a fast response time at pH = 4 with high sensitivity and selectivity. Linear correlation between F_0/F and the concentration was seen in the range of 0.2–18 μM and 0.2–25 μM for Sn^{4+} and Mo^{6+}, respectively. Under optimum condition, the limit of detection (LOD) for Sn^{4+} and Mo^{6+} were 150 nM and 132 nM, respectively. The performance of the sensor was evaluated by different real samples such as tap, river and mineral water, canned fish sample and tomato samples.

Introduction

Determination of tin in environmental, food and biological samples is important, since it can be toxic at high levels but is essential for humans at trace levels. There are mainly two chemical species of inorganic tin (Sn^{2+} and Sn^{4+}) in samples. Different forms of an element have different toxicities and therefore, development of new analytical methods for monitoring of inorganic tin species is extremely important.

Various instrumental techniques have been employed for the determination of tin species in different real samples, including electrochemical methods [1–4], atomic absorption spectrometry [4–8], inductively coupled plasma mass spectrometry [9], laser induced–breakdown spectroscopy [10], atomic fluorescence spectrometry [11], X-ray fluorescence spectrometry [12], phosphorimetry [13] and fluorimetric methods [14–17].

Molybdenum is a valuable alloying agent and use in alloys, electrodes, catalysts, circuit boards and in microwave devices and heat sinks for solid-state devices. It is an essential element in low concentrations especially in plants because of its important role in enzymatic redox reactions, but can be highly toxic at large concentrations [18]. Several techniques were used for determination of molybdenum such as X-ray fluorescence spectrometry [18], flame atomic absorption spectrometry [19], inductively coupled plasma [20], inductively coupled plasma mass spectrometry [21], spectrofluorimetry [22–26] and adsorptive stripping voltammetry [27, 28]. These methods require complicated sample preparation and sophisticated instruments which limit their applications. Thus, it is still of great challenge to develop sensitive, selective and environmentally friendly methods for ion sensing.

Semiconductor quantum dots (QDs) have attracted much attention in recent years. However, most traditional QDs contain heavy metal elements, which are toxic and environmentally hazard. Fluorescent carbon dots are the best candidates due to their low toxicity, excellent photostability, high selectivity and good water solubility.

Carbon dots (CD) can be generally synthesized by different methods. Electrochemical, laser ablation and arc discharges are top-down methods in which carbon dots are prepared from larger molecules. In bottom-up methods such as combustion/

✉ Reza Tabaraki
rezatabaraki@yahoo.com; r.tabaraki@ilam.ac.ir

[1] Department of Chemistry, Ilam University, Ilam, Iran

thermal, supported synthetic and microwave, carbon dots are prepared from molecular precursors [29]. Microwave-assisted techniques have advantages such as faster preparation, good reproducibility and stability of nanoparticles. Doping of carbon dots with heteroatoms N, S, P and B) can improve the fluorescence efficiency and selectivity. Co-doping of carbon dots with more heteroatoms lead to better sensing [30].

In this study, water-soluble boron and nitrogen-co-doped carbon dots (B-N-CDs) was prepared by microwave-assisted method using citric acid, boric acid and urea as carbon, boron and nitrogen sources. The B-N-CDs was successfully applied to the fluorescent determination of Sn^{4+} and Mo^{6+} ions in real samples with high sensitivity and selectivity.

Material and Methods

Chemicals

All chemicals were analytical grade and purchased from Merck. Stock solutions of Sn^{4+}, Mo^{6+}, interference ions and molecules (10 mM) were prepared with ultrapure water from the respective salts. Desired pH value was adjusted by using 0.01 M of universal buffer (a mixture of 0.04 M boric acid, 0.04 M phosphoric acid and 0.04 M acetic acid).

Preparation of Boron-Nitrogen-Co-Doped Carbon Dots

The boron-nitrogen-co-doped carbon dots were prepared by a simple and green microwave-assisted method [31]. Citric acid, boric acid and urea (each one 1 g) were dissolved in 20 mL of deionized water. Filtered solution was heated in a microwave oven at 700 W for 4 min. Resulting solid was dissolved in 20 mL water, filtered and evaporated until dry at room temperature. After washing of solid, it was re-dissolved in water and final concentration was 3 mg/mL. The fluorescence intensity of this CDs solution at $\lambda_{emission}$ = 455 nm and $\lambda_{excitation}$ = 350 nm was out of range; therefore it was diluted 10 fold. CDs dosage, excitation and emission slit widths must be optimized. 100 μL of this diluted solution was added to 3 mL of universal buffer. At excitation slit width = 5 nm and emission slit width = 10 nm, fluorescence intensity was also out of range. Different volumes of CDs solution and slit widths were checked until fluorescence intensity of CDs solution reached to 900 a.u (maximum of instrumental scale). This fluorescence intensity was obtained when 150 μL of diluted CDs was added to 3 mL of universal buffer in sample cell and excitation and emission slit widths were 2.5 nm and 5 nm, respectively.
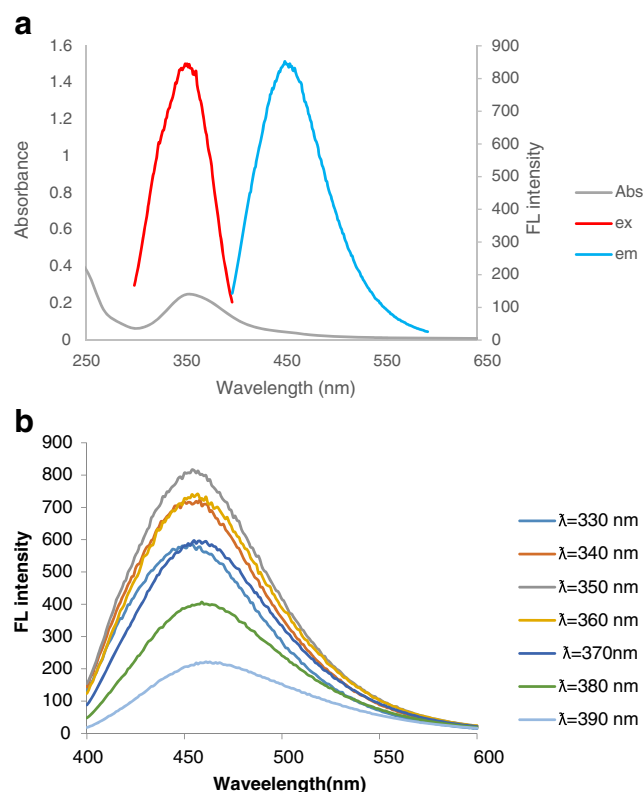

Fig. 1 a UV–vis absorption, excitation and emission spectra of CDs in aqueous solutions (3.0 mg mL^{-1}), λ_{ex} = 350 nm and λ_{em} = 455 nm (B) FL spectra at different excitation wavelength
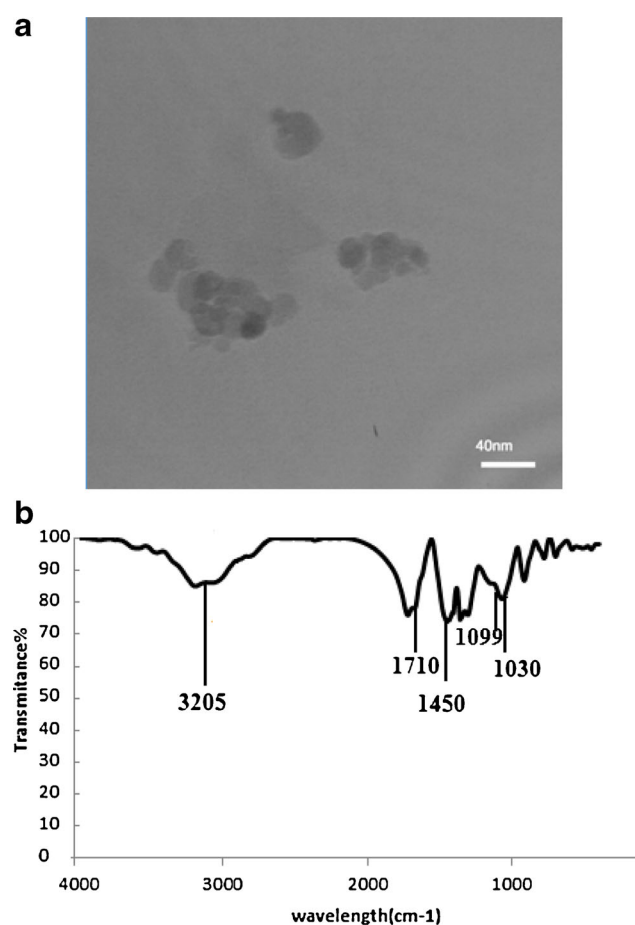
Fig. 2 a The typical HRTEM image of the B-N-CDs. b FT-IR spectrum of B-N-CDs

Instrumentation and Characterization

Varian Cary 300 Bio UV-Vis, Vertex 70 Fourier transformed infrared and Varian Cary spectrofluoremeter were used for UV-Vis, FT-IR and fluorescence spectral analysis. The size and morphology of the B-N-CDs were determined by MC30 high resolution transmission electron microscope (HRTEM; Philips) operated at 80 kV.

Spectrofluorometric Measurements

In a typical assay, 150 μL of B-N-CDs, 3 mL of universal buffer (pH = 4, 0.01 M) and appropriate volume of Sn^{4+} or Mo^{6+} solution were mixed and the fluorescence was measured immediately (1-cm quartz cuvette, $\lambda_{emission}$ = 455 nm, $\lambda_{excitation}$ = 350 nm, excitation slit width = 2.5 nm and emission slit width = 5 nm). All experiments were performed at room temperature. Selectivity experiments were done in a similar way by adding other ions instead of Sn^{4+} or Mo^{6+}.

Real Sample Analysis

Real water samples (river, mineral and tap water) were filtered through a 0.45 μm filtered membrane and then centrifuged at 4000 rpm for 15 min. Spiked water samples then analyzed with the proposed method.

Canned fish sample (1.0 g) was transferred into a 100-mL Erlenmeyer flask and 15 mL concentrated sulfuric acid and 3 mL $HClO_4$ were added. The solution was gently heated for
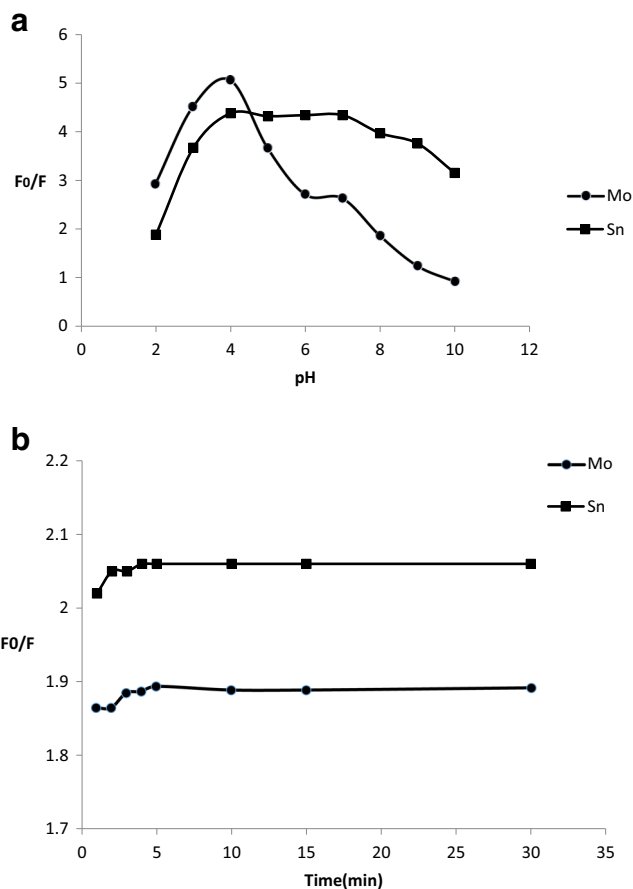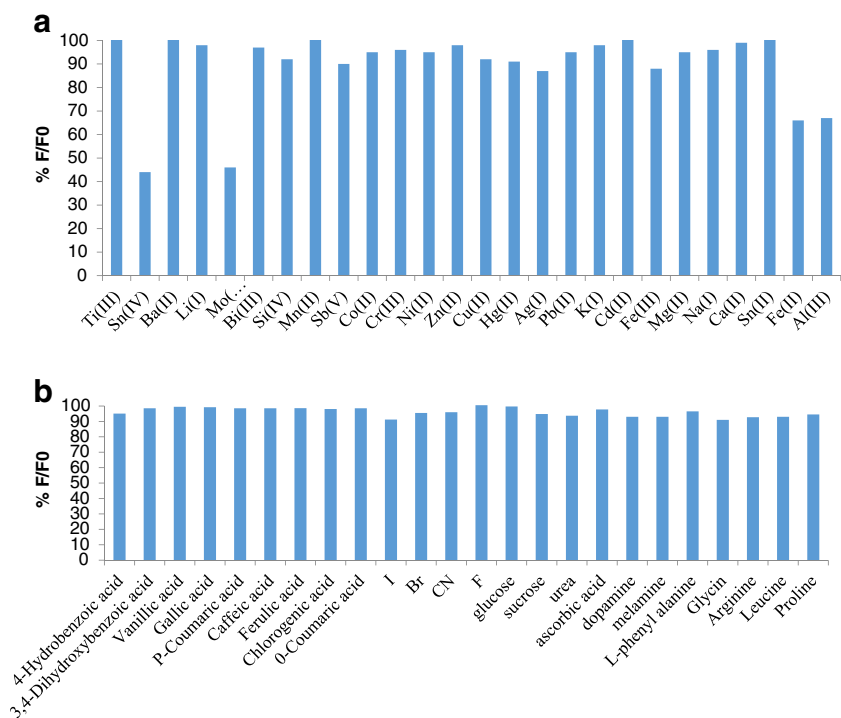
Fig. 4 Influence of pH **a** and time **b** on the relative florescence intensity in the presence of 20 μM Sn^{4+} or Mo^{6+}

Fig. 3 Fluorescence responses of B-N-QDs system to different ions and molecules (concentration was 20 μM)

sample digestion until no gas was evaporated. Then, 2 mL sulfuric acid and HNO₃ were added and again heated. Afterwards, it was cooled; its pH was adjusted with NaOH and filtered. The filtrate was collected in a 100-mL volumetric flask and diluted to the volume with water.

Tomato sample was first crushed and then heated for 3 h at 300 °C. After cooling, 1.0 g of the residual was carefully moistened with 4 mL of nitric acid and the mixture was heated on a hotplate to near dryness. The residue was diluted in a 25 mL volumetric flask. The solution was filtered through a 0.45 μm membrane filter and then centrifuged at 4000 rpm for 20 min [27].

Result and Discussion

Characterization of Boron-Nitrogen-Doped Carbon Dots (B-N-CDs)

UV–Vis and fluorescence spectra of the water-soluble B-N-CDs were shown in Fig. 1a. As shown, there were
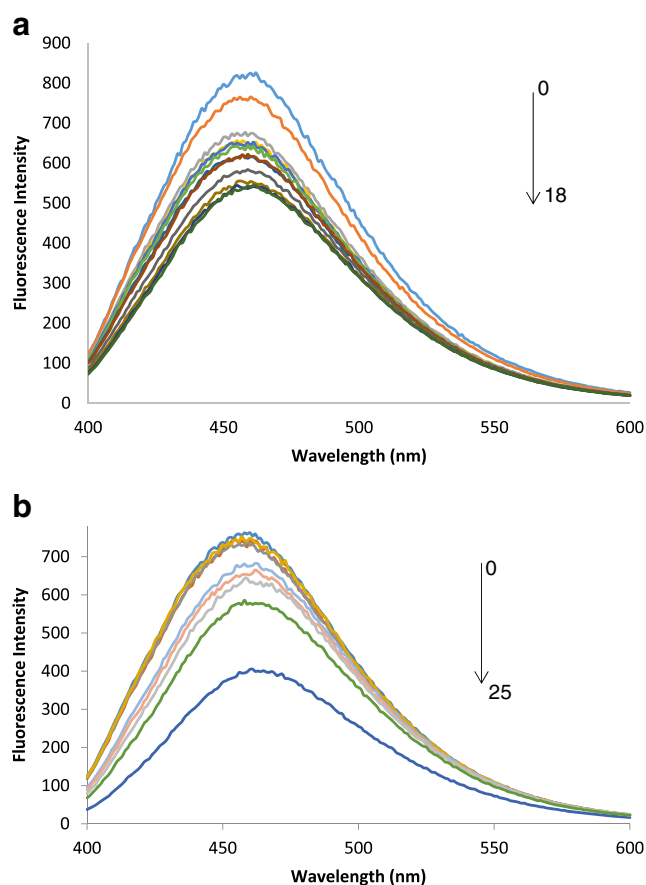
two absorption peaks located at 250 and 350 nm and absorption peak at 350 nm is related to the electron transitions from $\pi \rightarrow \pi^*$ of aromatic system. Sections of molecules which can undergo detectable electron transitions can be referred to chromophores. Auxochromes with free electron pairs have $n \rightarrow \pi^*$ transitions. In this work, both transitions occur because of presence of N atoms and aromatic system in B-N-CD structure. The presence of C = C and nitrogen atom in CD structure were verified by X-ray photoelectron spectroscopy in ref. 31. B-N-CDs had an excitation peak around 350 nm and when excited at this wavelength, exhibited strong fluorescence emission centered at 455 nm (Fig. 1a). The fluorescence intensity of the B-N-CDs also changes with the change of excitation wavelength from 330 to 390 nm (Fig. 1b) without obvious shift.

As shown in Fig. 2a, B-N-CDs were well dispersed with a diameter of about 20 nm based on high resolution transmission electron microscopy image of B-N-CDs. Next, FT-IR was also used to identify functional groups of the B-N-CDs surface (Fig. 2b). The absorption bands for O–H, N–H and carbonyl groups vibrations appeared at 3205 and 1710 cm⁻¹, respectively. These groups improve the hydrophilicity. B–O stretching vibration had absorption band at 1450 cm⁻¹. Absorption band at 1030 cm⁻¹ is also assigned to B–O–C bonding. B–N with sp³ bonding appears at 1099 cm⁻¹ [31].

Table 1 Comparison of the proposed fluorescence sensor with the some previously reported methods

Method	Detection limit (μg/L)	Linear range(μg/L)	Reference
Sn⁴⁺			
Differential pulse polarography	1510	10,000–40,000	[1]
Bismuth film electrode	16.6	20.2–929	[3]
Cloud point- AAS	12.6	46–750	[5]
Graphite furnace AAs	0.013	0.05–4	[6]
HG-MF-AAS	7.1	50–1000	[8]
SIA	380	1000–10,000	[14]
Spectrofluorimetric	2	10–800	[16]
B-N carbon dots	17.8	23.7–2137	This study
Mo⁶⁺			
Cloud point AAS	2.2	7.5–1800	[19]
Quadrupole ICP-MS	-	1–20	[21]
Spectrofluorimetric	10	100–900	[24]
Catalytic spectrofluorimetric	0.04	0–3	[25]
Derivative synchronous spectrofluorimetric	3.2	50–250	[26]
	49	500–4000	
Catalytic adsorptive stripping voltammetry	0.006	0.01–21	[27]
SIA	21	80–1920	[32]
B-N carbon dots	12.5	19–2400	This study

Fig. 5 Fluorescence emission spectra of the B-N-CDs in aqueous solution upon addition of various concentrations of **a** Sn⁴⁺ (from top to bottom: 0, 0.2, 0.8, 1, 2, 4, 6, 8, 12, 14, 16 and 18 μM), **b** Mo⁶⁺ (from top to bottom: 0, 0.2, 0.5, 1, 3, 5, 8,10,12,15,18, 20, 25 μM),excitation at 350 nm

Selectivity of B-N-CDs

Effect of different cations, anions and molecules on the fluorescence quenching of B-N-CDs were investigated (Fig. 3). Different ions were added into the B-N-CDs solution with a final concentration of 20 μM and then F/F_0 ratio was recorded. As shown, ratio decreased remarkably after addition of Sn^{4+} and Mo^{6+} ions, whereas other ions and molecules had negligible effects except Fe(II) and Al(III). B-N-CDs have only a small negative surface charge, probably due to the presence of charged borate ester bridges [31]. Thus, anions had no significant effect on the fluorescence of B-N-CDs because of repulsive forces.

Effect of pH and Time

Effect of pH on the fluorescence quenching of B-N-CDs were studied in the presence of 20 μM Sn^{4+} or Mo^{6+} ions. Relative fluorescence intensity increased by increasing pH and reached to maximum at pH = 4.0 and then decreased (Fig. 4a). The effect of time on the relative fluorescence intensity was studied at room temperature. As shown in Fig. 4b, fluorescence quenching was fast after addition of Sn^{4+} or Mo^{6+} ions. The results showed that this probe had a fast response time that is one of the important characteristic of good chemical sensors.

Performance Evaluation

Effects of different concentrations of Sn^{4+} and Mo^{6+} on the fluorescence spectrum of B-N-CDs were studied under the optimized conditions (Figs. 5a, b). Relative fluorescence intensity (F_0/F) of B-N-CDs linearly decreased by increasing Sn^{4+} and Mo^{6+} concentration in the range of 0.2–18 μM and 0.2–25 μM, respectively. This behavior could be described by the Stern-Volmer eq. ($F_0/F = K_{sv}[C] + 1$), where F_0 and F are the fluorescence intensities recorded in absence and presence of Sn^{4+}, respectively, [C] is the concentration of Sn^{4+} and K_{sv} is the Stern-Volmer quenching constant.

$$F_0/F = 0.0189\, C_{Sn4+}(\mu M) + 1.19\,(R^2 = 0.98) \qquad (1)$$

$$F_0/F = 0.057\, C_{Mo6+}(\mu M) + 1.09\,(R^2 = 0.99) \qquad (2)$$

Limit of detection (LOD) for Sn^{4+} and Mo^{6+} were evaluated to be 150 and 132 nM, respectively (LOD = 3σ/s, where σ and s are standard deviation of blank ($n = 5$) and slope of the calibration plot). These detection limits suggests that B-N-CDs will have very promising application in the detection of Sn^{4+} and Mo^{6+}. Table 1 summarizes the detection limit and linear range of different methods for determination of Sn^{4+} and Mo^{6+}. Advantages of this method are simple and green preparation method, easy performance, available and low cost reagents and no need to expensive instruments. Linear dynamic ranges were better than the most of other methods. Methods with better sensivities had limited dynamic ranges.

Real Sample Analysis

Performance of the B-N-CDs-based sensor was tested by tap, river and mineral water samples, canned fish sample and

Table 2 Determination of Sn^{4+} in different real samples

Samples	added (μM)	found[a] (μM)	Recovery (%)	RSD
Tap water	0	N.D.[b]	-	
	8	8.18 ± 0.02	102	0.94
	18	19.09 ± 0.03	105	1.85
	20	20.00 ± 0.04	100	3.23
River water	0	N.D.	-	
	8	8.13 ± 0.02	101	1.37
	18	17.47 ± 0.02	97	2.10
	20	21.21 ± 0.02	105	1.62
Mineral water	0	N.D.	-	
	8	8.00 ± 0.05	100	4.58
	18	8.00 ± 0.03	100	2.75
	20	17.15 ± 0.02	95	1.65
Canned fish	0	85.17		
	8	8.49 ± 0.07	105	3.51
	10	9.40 ± 0.05	95	2.50
	18	17.92 ± 0.10	99	4.70
	20	20.75 ± 0.02	103	0.94

[a] Average of three replicate measurement ± standard deviation
[b] N. D: not detected

Table 3 Determination of Mo^{6+} in different real samples

Samples	added (μM)	Found[a] (μM)	Recovery (%)	RSD
Tap water	0	N.D.[b]	-	
	10	9.67 ± 0.51	97	5.20
	20	20.07 ± 0.39	100	1.90
	40	42.2 ± 0.71	106	1.60
Mineral water	0	N.D.[b]	-	
	10	9.4 ± 0.36	94	3.60
	20	19.20 ± 0.21	96	1.10
	40	42.28 ± 0.33	105	0.70
River water	0	N.D.[b]	-	
	10	9.1 ± 0.14	91	1.50
	20	20.14 ± 0.19	101	0.90
	40	41.2 ± 0.44	103	1.06
Tomato	0	3.15		
	10	13.95 ± 0.18	105	1.66
	20	24.12 ± 0.21	104	1.00
	40	44.21 ± 0.32	102	0.75

[a] Average of three replicate measurements ± standard deviation
[b] N. D. not detected

tomato. The samples were spiked with Sn^{4+} or Mo^{6+} at different concentration levels and then analyzed with the proposed method (Tables 2 and 3). The recoveries were satisfactory. These results demonstrated that this sensor has the great potential in practical applications.

Conclusions

Water-soluble boron-nitrogen-doped carbon dots (B-N-CDs) was used for the trace detection of Sn^{4+} and Mo^{6+}. The linear ranges of B-N-CDs for Sn^{4+} and Mo^{6+} were 0.2–18 and 0.2–25 μM, respectively; while the limits of detection were 150 and 132 nM, respectively. Therefore, B-N-CDs can be used as fluorescence turn-off probes for the detection of Sn^{4+} and Mo^{6+} ions in real samples with a high sensitivity and selectivity.

References

1. Hubert C, Ziémons E, Rozet E, Breuer A, Lambert A, Jasselette C, De Bleye C, Lejeune R, Hubert P (2010) Development and validation of a quantitative method for the selective determination of tin species in tin octoate by differential pulse polarography. Talanta 80:1413–1420
2. Pérez-Herranz V, Garcia-Gabaldón M, Guiñón JL, Garcia-Antón J (2003) Effect of citric acid and hydrochloric acid on the polarographic behaviour of tin application to the determination of tin(II) in presence of tin(IV) in the activating solutions of the electrode less plating of polymers. Anal Chim Acta 484:243–251
3. Frena M, Campestrini I, de Braga OC, Spinelli A (2011) In situ bismuth-film electrode for square-wave anodic stripping voltammetric determination of tin in biodiesel. Electrochim Acta 56:4678–4684
4. Chomisteková Z, Culková E, Vojtko J, Brescher R, Tomčík P (2015) Voltammetric behavior of $I_2/2I^-$ redox system on boron-doped diamond electrode in various media and its utilization for the indirect detection of tin(II). J Electroanal Chem 758:46–53
5. Gholivand MB, Babakhanian A, Rafiee E (2008) Determination of Sn(II) and Sn(IV) after mixed micelle-mediated cloud point extraction using polyoxometalate as a complexing agent by flame atomic absorption spectrometry. Talanta 76:503–508
6. Uluozlu OD, Tuzen M (2015) Carrier element-free coprecipitation and speciation of inorganic tin in beverage samples and total tin in food samples using N-benzoyl-N,Ndiisobutylthiourea and its determination by graphite furnace atomic absorption spectrometry. LWT Food Sci Technol 63:1091–1096
7. Prusa L, Dedina J, Kratzer J (2013) Ultratrace determination of tin by hydride generation in-atomizer trapping atomic absorption spectrometry. Anal Chim Acta 804:50–58
8. Galazzi RM, Arruda MAZ (2013) Optimization of a hydride generation metallic furnace atomic absorption spectrometry (HG-MF-AAS) method for tin determination: analytical and morphological parameters of a metallic atomizer. Talanta 117:543–548
9. Wolf SF, Compton JR, Gagnon CJL (2012) Determination of 11 major and minor elements in chondritic meteorites by inductively coupled plasma mass spectrometry. Talanta 100:276–281
10. Carricondo J, Iofrida M, Ararat C, Iribarren M, Corvalán C (2015) Laser induced–breakdown spectroscopy for quantitative Sn analysis in Zr based alloys. Procedia Mater Sci 9:129–134
11. Jiang X, Gan W, Wan L, Deng Y, Yang Q, He Y (2010) Electrochemical hydride generation atomic fluorescence spectrometry for detection of tin in canned foods using polyaniline-modified lead cathode. J Hazard Mater 184:331–336
12. Figi R, Nagel O, Tuchschmid M, Lienemann P, Gfeller U, Bukowiecki N (2010) Quantitative analysis of heavy metals in automotive brake linings: a comparison between wet-chemistry based analysis and in-situ screening with a hand-held X-ray fluorescence spectrometer. Anal Chim Acta 676:46–52
13. Jiaming L, Guohui Z, Tianlong Y, Aihong W, Yan F, Longdi L (2003) Determination of trace tin by solid substrate-room temperature phosphorimetry using sodium dodecyl sulfate as sensitizer. Spectrochim Acta Part A 59:2081–2085
14. Boa Morte ES, Grac M, Korn A, Saraiva MLMFS, Lima JLFC, Pinto PCAG (2009) Sequential injection fluorimetric determination of Sn in juices of canned fruits. Talanta 79:1100–1103
15. Zhu L, Yang J, Wang Q, Zeng L (2014) Highly selective fluorescent probe for the detection of tin(IV) ion. J Lumin 148:161–164
16. Manzoori JL, Amjadi M, Abolhasani D (2006) Spectrofluorimetric determination of tin in canned foods. J Hazard Mater 137:1631–1635
17. Yazid SNAM, Chin SF, Pang SC, Ng SM (2013) Detection of Sn(II) ions via quenching of the fluorescence of carbon nanodots. Microchim Acta 180:137–143
18. Das AK, Chakraborty R, Cervera ML, Guardia M (2007) A review on molybdenum determination in solid geological samples. Talanta 71:987–1000
19. Gurkan R, Aksoy U, Ulusoy HI, Akcay M (2013) Determination of low levels of molybdenum (VI) in food samples and beverages by cloud point extraction coupled with flame atomic absorption spectrometry. J Food Compos Anal 32:74–82
20. Agrawal YK, Sharma KR (2005) Speciation, liquid–liquid extraction, sequential separation, preconcentration, transport and ICP-AES determination of Cr(III), Mo(VI) and W(VI) with calix-crown hydroxamic acid in high purity grade materials and environmental samples. Talanta 67:112–120
21. Reid HJ, Bashammakh AA, Goodall PS, Landon MR, O'Connor C, Sharp BL (2008) Determination of iodine and molybdenum in milk by quadrupole ICPMS. Talanta 75:189–197
22. Jiang C, Wang J, He F (2001) Spectrofluorimetric determination of trace amounts of molybdenum in pig liver and mussels. Anal Chim Acta 439:307–313
23. Capitan F, Sanchez-Palencia G, Naval A, Capitan-Vallvey LF, Vilchez JL (1992) Simultaneous determination of molybdenum and tungsten by first-derivative synchronous solid-phase spectrofluorimetry. Anal Chim Acta 259:345–353
24. Blanco CC, Campana AG, Barrero FA, Ceba MR (1993) Simultaneous spectrofluorimetric determination of traces of molybdenum and boron in plant leaves. Anal Chim Acta 283:213–223
25. Kawakubo S, Suzuki H, Iwatsukic M (1996) Catalytic spectrofluorometric determination of ultratrace molybdenum in natural fresh water. Anal Sci 12:767–771
26. Blanco CC, Campana AG, Barrero FA, Ceba MR (1995) Micellar medium for the analysis of complex mixtures of molybdenum and tungsten by derivative synchronous spectrofluorimetry in steels. Talanta 42:1037–1044
27. Ensafi AA, Khaloo SS (2005) Determination of traces molybdenum by catalytic adsorptive stripping voltammetry. Talanta 65:781–788
28. Deng P, Fei J, Zhang J, Feng Y (2011) Determination of molybdenum by adsorptive anodic stripping voltammetry of molybdenum–alizarin violet complex at an acetylene black paste electrode. Food Chem 124:1231–1237
29. Baker SN, Baker GA (2010) Luminescent carbon nanodots: emergent nanolights. Angew Chem Int Ed 49:6726–6744

30. Wang Y, Kim SH, Feng L (2015) Highly luminescent N, S-co-doped carbon dots and their direct use as mercury (II) sensor. Anal Chim Acta 890:134–142

31. Bourlinos AB, Trivizas G, Karakassides MA, Baikousi M, Kouloumpis A, Gournis D, Bakandritsos A, Hola K, Kazak O, Zboril R, Papagiannouli I, Aloukos P, Couris S (2015) Green and simple route toward boron doped carbon dots with significantly enhanced non-linear optical properties. Carbon 83:173–179

32. Lesková M, Sklenárová H, Bazel Y, Chocholous P, Solich P, Andruch V (2012) A non-extractive sequential injection method for determination of molybdenum. Talanta 96:185–189